

# Determination of Molecular Parameters of Linear and Circular Scleroglucan Coexisting in Ternary Mixtures Using Light Scattering

Marit Sletmoen,<sup>†</sup> Erik Geissler,<sup>‡</sup> and Bjørn T. Stokke<sup>\*,†</sup>

Biophysics and Medical Technology, Department of Physics, The Norwegian University of Science and Technology, NTNU, NO-7491 Trondheim, Norway, and Laboratoire de Spectrométrie Physique CNRS UMR 5588, Université Joseph Fourier de Grenoble, B.P.87, 38402 St Martin d'Heres, France

Received December 23, 2005; Revised Manuscript Received January 19, 2006

A combination of static and dynamic light scattering (SLS and DLS) is applied here to determine molecular parameters for coexisting linear and circular scleroglucan polymers of similar molecular weights, dissolved in water, that is, forming a ternary system. The weight-average molecular weights,  $M_w$ , were determined to be  $3.2 \times 10^5$  and  $3.9 \times 10^5$  g/mol for the circular and linear molecules, respectively, whereas the  $z$ -average radius of gyration,  $R_g$ , was found to be equal to 41 nm for the circular molecules and 136 nm for the linear ones. These values are within a physically reasonable range in view of the heterogeneity of the samples. This study confirms that decomposition of total scattering intensities deduced from the dynamic properties can be used to determine molecular parameters of populations of molecules of equal  $M_w$  but different morphologies present in ternary mixtures.

## Introduction

Scleroglucan is a (1→3)- $\beta$ -D-glucan polysaccharide produced by the fungus *Sclerotium*. Dissolved in water at room temperature, it adopts a linear, rigid, triple helical structure.<sup>1–4</sup> The persistence length,  $L_p$ , has been estimated to be about 150 nm.<sup>5</sup> Due to these structural features, scleroglucan and other (1→3)- $\beta$ -D-glucans are commonly used as a molecular model for the rodlike or stiff wormlike chain behavior.<sup>5,6</sup> The extended chain conformation is also taken to explain the high viscosity observed in solutions containing scleroglucan, which persists over a wide range of temperature, pH, and ionic strength. Changes of solvent conditions can be used to dissociate and reassociate the triple helix.<sup>2,7–10</sup> If the renaturation occurs at a high polymer concentration, large aggregates, and eventually gels, will form.<sup>11</sup> If the renaturation occurs at concentrations well below the critical concentration needed for gelation,  $C_0$ , and the chain length of the molecules lies within a certain interval, a fraction of the polymer strands will reassociate to form cyclic species.<sup>12–15</sup> The relative abundance of such cyclic species increases with decreasing concentration below  $C_0$ . Fractions rich in cyclic species have recently been characterized by atomic force microscopy (AFM) and size exclusion chromatography combined with a multiangle laser light scattering detector (SEC-MALLS).<sup>16</sup> The mass per unit length determined for the structures allowed us to conclude that the circular structures formed are composed of triple helices. If exposed to thermal annealing following the renaturation step, these circular and linear structures of scleroglucan are stable and do not alter their topology.<sup>17</sup>

The properties of solutions containing (1→3)- $\beta$ -D-glucans are highly dependent on the morphology of the molecules. The presence of circular species or aggregates affects both the

biological (i.e., immunostimulating) and physical properties (i.e., the intrinsic viscosity and gel forming properties) of scleroglucan preparations. Determination of the fraction of circular structures present in such solutions is therefore important. Ultramicroscopic techniques allow reliable determination of the fraction of linear, circular, and aggregated structures,<sup>15,16,18</sup> but these techniques are time-consuming. The aim of this paper is to investigate the potential of dynamic light scattering (DLS) to provide information related to the morphology of the molecules present in solutions of scleroglucan exposed to denaturing conditions and then renatured. More precisely, we investigate whether differences in dynamic properties allow linear and circular molecules coexisting in solutions of scleroglucan renatured at low polysaccharide concentrations to be characterized independently using light scattering.

Light scattering is a preferred method for molecular characterization of macromolecules in solution.<sup>19–21</sup> The weight-average molecular weight,  $M_w$ , and  $z$ -average radius of gyration,  $R_g$ , are two parameters determined by static light scattering (SLS). The hydrodynamic radius,  $R_H$ , on the other hand, is determined by dynamic light scattering (DLS). In purely diffusive systems where no additional molecular effects are present, the decay rate of the intensity correlation function reflects the diffusion of the molecules over a distance of  $1/q$ , where  $q = (4\pi/\lambda) \sin(\theta/2)$  is the transfer wavenumber, with  $\theta$  and  $\lambda$  being the scattering angle and the wavelength of the incident light in the sample medium, respectively. For particles of irregular shape, for example, polymer coils,<sup>22</sup> no simple relation exists between the diffusion coefficient and their geometrical size. A hydrodynamic radius for translational movement,  $R_H$ , may be assigned through the translational diffusion coefficient,  $D_T$ , by virtue of the Stokes–Einstein equation:

$$D_T = \frac{k_B T}{6\pi\eta_0 R_H} \quad (1)$$

\* Corresponding author. Fax: +47 73 59 77 10. E-mail: bjorn.stokke@phys.ntnu.no.

<sup>†</sup> The Norwegian University of Science and Technology.

<sup>‡</sup> Université Joseph Fourier de Grenoble.

In eq 1,  $k_B$ ,  $T$ , and  $\eta_0$  are the Boltzmann constant, absolute temperature, and solvent viscosity, respectively.

In aqueous solutions, both SLS and DLS measurements are challenging due to the precautions required to eliminate dust and possible intermolecular associations. Another challenge encountered with solutions of polysaccharides is related to their inherent polydispersity, which is a common feature for all populations of polysaccharides, although the degree of polydispersity can be reduced by chromatographic or related techniques. For polydisperse samples, the autocorrelation function obtained by DLS data is a superposition of many exponential curves. If the relaxation time is evaluated from the initial portion of the autocorrelation function, the corresponding value of the diffusion coefficient is the  $z$ -average.

Previous studies have shown that the properties of molecules present in dilute solutions that contain more than one polymer component, each having different hydrodynamic properties, can be deduced. Benmouna et al.<sup>23</sup> developed a formalism to treat the DLS spectrum of ternary polymer solutions in the semidilute regime. They show that the concentration auto-(time)-correlation function of the ternary polymer solution probed by DLS consists of a sum of two exponentially decaying functions. The position and amplitude of each exponential depend on polymer structure, polymer-solvent interaction, polymer blend composition, and the refractive index increments of both polymers relative to the solvent. Akcasu et al.<sup>24</sup> showed that interference between the fast and slow modes can occur even in the dilute regime. Only in the zero concentration limit does the coupling between the two modes disappear. Several later experiments have been carried out to compare with these theories. One such study focused on mixtures of two populations of polystyrene, of different molecular weights, in toluene.<sup>25</sup> The study shows that over a wide concentration regime the intensity correlation function of the solution exhibits a bimodal structure. In such multicomponent systems, the total intensity detected at each scattering angle is a sum of the contributions from all of the components in the mixture. If, in addition to the SLS measurements, DLS measurements are performed at each scattering angle, the fraction of the intensity scattered by each of the populations present in the mixture can be obtained. The determination requires that the difference in  $D_T$  of the components be sufficiently large for them to be resolved in the autocorrelation function by a deconvolution analysis, for example, CONTIN.<sup>26,27</sup> In this case, such an analysis allows populations of molecules to be identified, each characterized by their respective  $R_H$  value. When the relative scattering intensity is plotted against  $R_H$ , the area under a peak corresponding to a population of molecules of a given  $R_H$  value reflects the fraction of the scattered intensity due to that group of molecules. A combination of SLS and DLS measurements therefore allows the fraction of the total scattered intensity from each component to be identified at each scattering angle. From this information, the molecular parameters  $M_w$  and  $R_g$  can be determined for each component. A second requirement for this approach to work is that the relative fraction of the two species be known over the whole concentration range studied. For solid suspensions, as in granulometric measurements, this constraint is lifted by the fixed relationship that exists between  $M_w$  and  $R_H$  (i.e.,  $M_w \propto R_H^{D_f}$ , where the fractal dimension is  $D_f = 3$ ). For polymer solutions, however, an analogous relationship (with a different value of  $D_f$ ) is valid only when the components adopt the same type of conformation over the entire range of molecular weights. In ref 25, the fraction of each of the two polystyrene populations was known. Liu et al. investigated solutions

containing single molecules and their aggregates.<sup>28</sup> In this study, the polymer unimers (sulfonated poly(*p*-phenylene)) coexisted with large aggregates over the entire range of polymer concentrations explored, but the percentage of polyelectrolyte chains included in aggregates increased with increasing total polymer concentration. To determine the molecular parameters of the low molecular weight component, the hypothesis that  $D_f = 3$  would have had to be adopted for the aggregates.

In this work, we have performed static and dynamic light scattering measurements on solutions of the industrially important (1 $\rightarrow$ 3)- $\beta$ -D-glucan scleroglucan exposed to a denaturation-renaturation cycle. Such solutions can be considered as ternary systems containing linear and circular molecules of scleroglucan dissolved in water. The properties of solutions containing these polysaccharides are highly dependent on the morphology of the molecules. Even though the presence of linear, circular, and aggregated structures can be reliably determined by ultramicroscopic techniques,<sup>15,16</sup> these are time-consuming. The development of alternative techniques that can yield information concerning the circular and aggregated structures present in such mixtures is therefore of interest. The present paper investigates dilute ternary solutions with this aim in mind. All measurements are extrapolated to  $q = 0$  and zero concentration to eliminate interference effects between the two polymer components and thereby address the properties of the two components separately.

## Materials and Methods

### Sample Preparation. Preparation of Solutions Containing Dextrans.

In addition to the ternary solutions of linear and circular scleroglucan, the experimental procedure was evaluated using a two-component mixture of dextran of known  $M_w$ . In this test, dextran polymers were chosen with a hydrodynamic radius close to that of the scleroglucan species studied.

Three dextrans with different  $M_w$  values were studied. All were obtained from Sigma and received as a dry powder with nominal weight-average molecular weights of  $7 \times 10^4$ ,  $46.5 \times 10^4$ , and  $2 \times 10^6$  g/mol. The  $M_w$  value had been determined using low angle light scattering. Stock solutions, each containing dextran of a given nominal weight, were prepared by dissolving the powder in filtered MQ water. The concentrations of the stock solutions varied from 20 g/L for the low molecular weight dextran to 10 g/L for the highest molecular weight sample. Dilution series of a concentration that would result in a suitable scattered intensity were then prepared from each of the dextran solutions, by diluting the stock solution with filtered MQ water. Both the water and the stock solution were filtered directly through 0.2  $\mu$ m filters (Millipore) into the 10 mm diameter glass tubes used for the measurements. Dilution series containing two dextrans of different molecular weights were also prepared using the same stock solutions and filtering procedure. In these samples, the relative fractions of the two populations of dextrans were kept constant while changing the total polysaccharide concentration.

*Preparation of Solutions Containing Circular and Linear Scleroglucans.* The scleroglucan used was Actigum CS11 provided by Sanofi Bioindustries, France. The scleroglucan powder was dissolved in MQ water to a concentration of 10 g/L and left under stirring at 55 °C for  $\sim$ 4 h and then at room temperature for 3 days. The molecules present in the resulting solution were ultrasonically depolymerized (Braun Labsonic 1510, power 50 W, 4 mL aliquots) for 15 min in order to obtain a chain length within the interval that yields a large fraction of cyclic topology upon denaturation-renaturation. The  $M_w$  value and polydispersity of the molecules present in the resulting solution were determined by SEC-MALLS to be  $4.2 \times 10^5$  g/mol and  $1.4 \pm 0.1$ , respectively. A solution containing both circular and linear molecules of scleroglucan was prepared using experimental conditions that previously were shown to give a low fraction of aggregates and a high

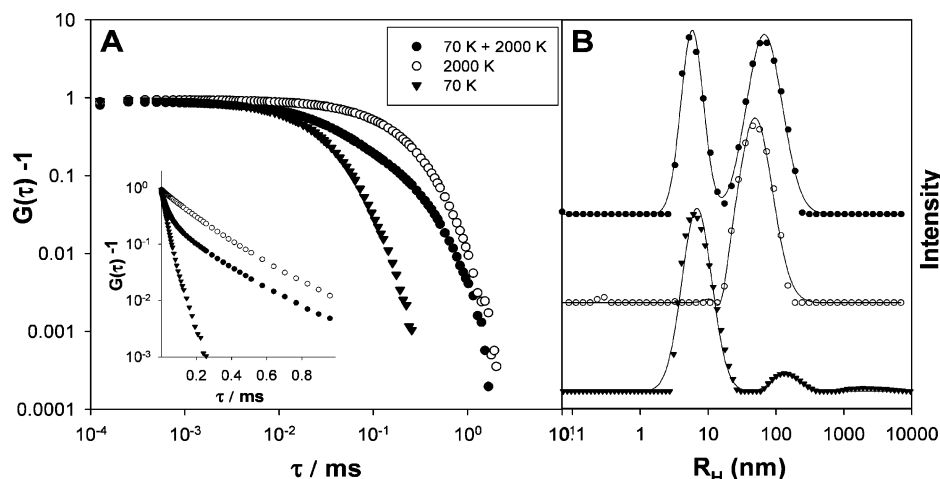


**Figure 1.** (A) Autocorrelation function obtained for solutions containing dextrans at the scattering angle  $120^\circ$ . Inset: semilogarithmic presentation of the autocorrelation functions. (B) CONTIN inverse Laplace transforms of DLS correlation functions from solutions containing dextran. The upper spectrum was obtained from a mixture of dextrans with a nominal molar mass of  $M_w = 7 \times 10^4$  g/mol and  $M_w = 2 \times 10^6$  g/mol. The middle and bottom spectra were obtained from solutions containing dextran with  $M_w = 2 \times 10^6$  g/mol (middle) and  $M_w = 7 \times 10^4$  g/mol (bottom). Continuous lines are least-squares fits to log-normal distributions (eq 2). These curves and their angular variation allow the absolute scattering intensity to be estimated and hence the molar mass and the radius of gyration of each component.

fraction of circles in the renatured sample.<sup>15,16</sup> The linear scleroglucan solution was diluted to 1 g/L, transferred to a dialysis tube (Medicell International,  $M_w$  cutoff for proteins: 12 000–14 000), and dialyzed against 0.5 M NaOH for 2 h at room temperature. The alkaline-treated sample was renatured by exposing it to a gradual decrease in pH, obtained by transferring the dialysis tube to a bath containing 0.1 M NaOH, pH to 11.9 heated to  $55^\circ\text{C}$ . The pH of the solution was adjusted by adding HCl. The polysaccharide solution in the tube was first dialyzed against this solution for 3 h and then against MQ water (pH 6.3) at room temperature overnight. After re-establishment of neutral conditions, the sample was heated to  $95^\circ\text{C}$  for 2 h and then allowed to cool in air, a thermal treatment reported to increase the structural stability of the circular species formed.<sup>17</sup> The molecular weight and the polydispersity index of this sample were determined by SEC-MALLS to be  $4.4 \times 10^5$  g/mol and  $1.6 \pm 0.05$ , respectively. The total concentration of polysaccharide present in the starting solution was determined both before and after filtering, using the phenol–sulfuric acid reaction.<sup>29</sup> A 14% loss due to the filtering was observed. Solutions containing from 4.75 to 0.95 mg of scleroglucan/mL were prepared for the light scattering experiments.

**Light Scattering.** Measurements were made with an ALV5000 correlator and ALV 5022F goniometer, equipped with fiber optic coupling and an avalanche diode, and a 22 mW HeNe laser working at 632.8 nm. The value of the refractive index increment,  $dn/dc$ , of scleroglucan/water was taken to be 0.14 mL/g.<sup>3</sup> For the angular dependence of the total scattered intensity, static light scattering (SLS) measurements were performed at  $23^\circ\text{C}$  at scattering angles between  $30$  and  $150^\circ$ . The dynamic light scattering (DLS) measurements were made in the same way but with longer counting times (300 s) to improve the signal-to-noise ratio of the correlation function. The DLS measurements on solutions containing two populations of polymers differing in molecular mass or morphology yielded autocorrelation functions in which two distinct diffusion modes could be resolved. The characteristic decay time distribution function,  $G(\tau)$ , was obtained from the normalized intensity autocorrelation function,  $g^{(2)}(t)$ , using the constrained regularization inverse Laplace transform program CONTIN.<sup>26,27</sup> Applying CONTIN analysis to the autocorrelation functions from a two-component system enables their respective diffusion modes to be determined unambiguously provided the diffusion times of the particles are sufficiently different. Each peak that appears in the distribution of macromolecular species as a function of hydrodynamic radius can be approximated rather well by a log-normal distribution. By fitting a sum of two log-normal functions to the spectra, an estimate is obtained of

the fraction of the total scattered intensity from each of the two components in the mixture:

$$I = I_1 + I_2 = I[\int G_1(\tau) d(\ln \tau) + \int G_2(\tau) d(\ln \tau)] \quad (2)$$

where  $\int G_1(\tau) d(\ln \tau) + \int G_2(\tau) d(\ln \tau) = 1$ . In eq 2,  $I$  is the total scattered intensity,  $I_1$  and  $I_2$  are the fraction of the total intensity due to the presence of components 1 and 2, respectively, and  $G_1(\tau)$  and  $G_2(\tau)$  are the log-normal components of each species in the distribution. The combined information obtained from SLS and DLS thus yields separate Zimm plots for each of the two populations of polysaccharides present in the mixtures.

**Atomic Force Microscopy.** The samples were prepared for atomic force microscopy (AFM) following a procedure reported elsewhere.<sup>30</sup> Aliquots of the samples were mixed with 60% aqueous glycerol to a final polysaccharide concentration of 2–4  $\mu\text{g/mL}$  and a final weight fraction of glycerol equal to 50%. A small volume of these solutions was sprayed on freshly cleaved mica disks and vacuum-dried at  $10^{-6}$  Torr for at least 2 h.

AFM topographs of scleroglucan were obtained using a Digital Instruments Multimode IIIa atomic force microscope equipped with an E-scanner. The instrument was operated in tapping mode using silicon TESP cantilevers (Digital Instruments, Santa Barbara, CA) with a nominal spring constant of 20–100 N/m and nominal resonance frequencies of 200–400 kHz.

## Results

**Combined DLS and SLS Measurements on Solutions Containing Dextrans.** The measurements on the dextran solutions were used as validation tests of the decomposition procedure described above. Dynamic light scattering measurements were performed on solutions containing dextrans with varying molecular weights as well as on mixtures of these. Unlike the samples containing dextran chains having the same reported  $M_w$  value, the DLS measurements on solutions containing two populations of polymers, differing in their reported  $M_w$  values, resulted in autocorrelation functions where two distinct diffusion modes are evident (Figure 1A). The spectra displayed in Figure 1B (dotted lines) are the result of the CONTIN analysis of the autocorrelation functions obtained for solutions containing low molecular weight dextran ( $M_w = 7 \times 10^4$  g/mol, bottom



**Table 1.** Light Scattering Parameters of Dextran Obtained from Measurements on Solutions Containing One or Two Components<sup>a</sup>

$M_{\text{nom}} \times 10^{-3}$ (g/mol)	$M_w \times 10^{-3}$ (g/mol)	$R_g$ (nm)	$R_H$ (nm)
components analyzed separately			
70	56	11.1	6.5
461	465	34.7	16.5
2000	1770	51.1	37.0
components analyzed in mixture			
70	57	4.9	6.0
2000	2127	49.8	48.7

<sup>a</sup>  $M_{\text{nom}}$  had been determined by the producer using low angle light scattering.  $M_w$  and  $R_g$  are based on CONTIN analysis of the autocorrelation functions from the two-component systems coupled with Zimm diagrams of the SLS data.  $R_H$  is obtained from CONTIN analysis of the autocorrelation functions from the two-component systems.

spectrum), high molecular weight dextran ( $M_w = 2 \times 10^6$  g/mol, middle spectrum), as well as a mixture of these polymers (upper spectrum). The continuous lines overlaid on the spectra are the least-squares fit of eq 2 to these data.

From the observed decay times, the hydrodynamic radii,  $R_H$ , of the dextran chains were determined. On the basis of SLS and DLS measurements of different dextran solutions, each containing one or two populations of dextran molecules characterized by a known nominal  $M_w$  value, Zimm plots were obtained (not shown). Mixtures containing dextran with a molecular weight of  $7 \times 10^4$  and  $2 \times 10^6$  g/mol yielded estimates for the molecular weights that coincided with those measured separately with an error of less than 5% (Table 1).

**Combined DLS and SLS Measurements on Solutions Containing Linear and Circular Scleroglucans.** Figure 2A is an AFM topograph showing the structures present in the scleroglucan solution prior to the denaturation–renaturation treatment. The polydispersity index of these linear scleroglucan topologies before exposure to denaturing conditions was determined by SEC-MALLS to be  $M_w/M_n = 1.4 \pm 0.07$ .<sup>16</sup> For the same sample after denaturation–renaturation (Figure 2B), a polydispersity index of  $M_w/M_n = 1.6 \pm 0.05$  was observed.<sup>16</sup> The structures appearing on the AFM topographs in Figure 2B were counted as being either linear or circular. Applying this approach on a number of AFM topographs, depicting a total of 249 molecules, determined the fraction of linear molecules to be 50% of the total number of molecules appearing on the images.

DLS measurements were made for solutions containing scleroglucan exposed to a denaturation–renaturation cycle (Figure 3). The autocorrelation function obtained from DLS measurements on this solution allowed separation into two distinct diffusion modes, indicating the presence of two dynamically separable populations of particles. The Zimm representations of the fast and slowly diffusing fractions, presented in Figure 4, show appreciable dispersion in the data. Simultaneous fitting to all of the data points in the Zimm procedure helps to reduce this noise, thereby yielding  $M_w$  and  $R_g$  values for the two populations of molecules. The results are summarized in Table 2. Using the observation that the fraction of circular molecules is 50% of the total number of molecules present in the solution, the  $M_w$  value of the fast diffusing structures was  $(3.2 \pm 0.2) \times 10^5$  g/mol. The radius of gyration and hydrodynamic radius of these structures, on extrapolation to zero scattering angle and zero concentration, were found to be  $R_g = 41 \pm 7$  nm and  $R_H = 15 \pm 1$  nm, respectively. For the population of slowly diffusing molecules, the Zimm plot yielded  $M_w = (3.9 \pm 1.0) \times 10^5$  g/mol.  $R_g$  and  $R_H$  for this population were determined to be  $136 \pm 18$  and  $92 \pm 11$  nm, respectively.

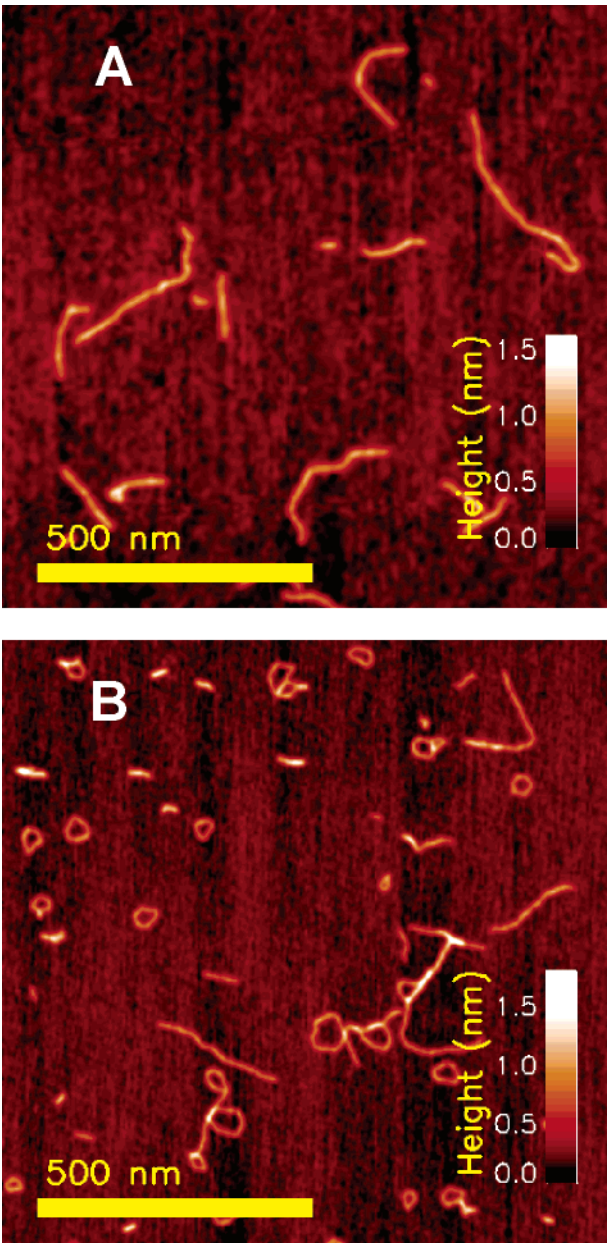


**Figure 2.** Tapping-mode AFM height topographs of scleroglucan before (A) and after (B) exposure to a denaturation–renaturation cycle. Note the coexistence of various molecular topologies present in the renatured sample (B).

**Table 2.** Light Scattering Parameters of Scleroglucan Solutions Containing Structures with Different Morphologies

morphology	$M_w \times 10^{-3}$ (g/mol)	$R_g$ (nm)	$R_H$ (nm)	$\rho$
circular	$320 \pm 20$	$41 \pm 7$	$15 \pm 1$	$2.7 \pm 0.5$
linear	$390 \pm 100$	$136 \pm 18$	$92 \pm 11$	$1.50 \pm 0.25$

It should be noted that the analysis of the autocorrelation function for some of the data gave rise to significantly higher apparent hydrodynamic radii for the slowly diffusing structures. As discussed below, the spread in the observed diffusion time is probably due to not only the polydispersity of the sample but also the occasional formation of entanglements between the linear molecules at the actual concentration. In an attempt to describe the hydrodynamic radius of single linear molecules, and not their entanglements, the highest observed values were excluded from the analysis when determining  $R_H$  for the slowly diffusing structures.

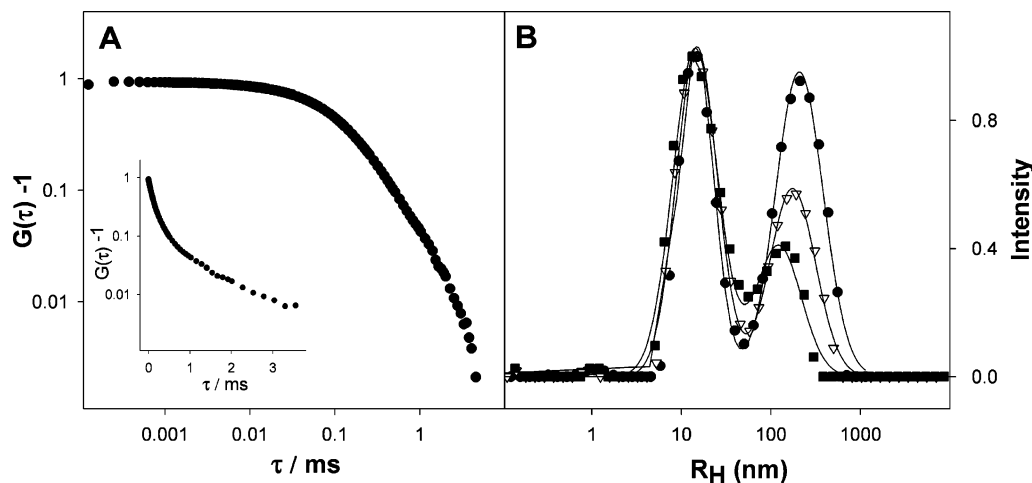


**Figure 3.** (A) Autocorrelation function obtained for solutions containing circular and linear molecules of scleroglucan. Inset: Semilogarithmic presentation of the autocorrelation functions. (B) CONTIN analysis of DLS spectra from the sample containing circular and linear molecules of scleroglucan. The relative amplitudes of the peaks of the fast and slowly diffusing structures change with scattering angle. The spectra shown are obtained at scattering angles of 30° (filled circles), 70° (open triangles), and 130° (filled squares). The continuous lines are the fits of eq 1 to the experimental data.

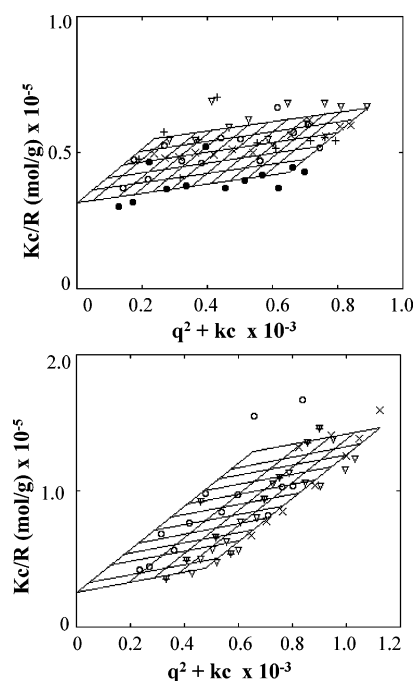


**Figure 4.** Zimm plots from measurements performed on mixtures containing linear and circular scleroglucan molecules. The upper plot is based on the fraction of the light scattered by the fast diffusing structures ( $R_H = 15 \pm 1$  nm, see Figure 3), and the lower plot shows the data for the slowly diffusing structures ( $R_H = 92 \pm 11$  nm, see Figure 3).

### Discussion

The control experiments on dextran are in agreement with previous studies,<sup>25</sup> showing that  $M_w$ ,  $R_g$ , and  $R_H$  can be determined in a ternary polymer solution provided the relaxation times of the two components can be resolved and the concentration of each is sufficient to yield a detectable signal. Alternative methods developed to analyze the intensity autocorrelation data might give rise to a higher resolution in bimodal distributions than that obtained with CONTIN.<sup>31</sup> The use of such programs could thus further improve the resolution in the spectra presented in Figure 3B. Still, on the basis of the observations and the arguments presented below, we conclude that the use of the CONTIN program and the presented procedure did allow two

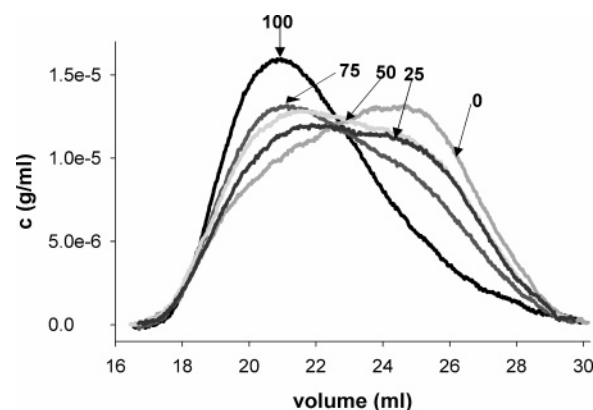


**Figure 5.** Elution profiles as a function of elution volume for native, linear scleroglucan and for the scleroglucan sample exposed to a denaturation–renaturation cycle as well as for mixtures of these two samples characterized by the content (%) of the native sample. Data adapted from those originally reported by Sletmoen et al.<sup>16</sup>

populations of molecules with different relaxation times to be resolved both in the three-component dextran solutions and in the renatured scleroglucan solutions.

Unlike mixtures of linear flexible polymers of different molecular weights, the  $M_w$  value for the scleroglucan solution cannot be determined on the basis of a simple power law relation between  $M$  and  $R_H$ . The reason for this is that the persistence length of 150 nm<sup>5,32</sup> corresponds to a molecular weight of 330 000 g/mol; below this mass, the chain behaves almost as a stiff rod. At higher  $M$ , the chain flexibility manifests itself as a deviation from rodlike behavior. The molecular weight range of the scleroglucan molecules in the sample studied therefore extends from rodlike, where  $M$  is proportional to  $R_H$ , to semiflexible behavior, where  $M$  depends more strongly on  $R_H$ . In the scleroglucan sample studied here, the presence of the circular structures makes this approach even more challenging. The  $M_w$  and  $z$ -average  $R_g$  values of the scleroglucan molecules were thus instead determined from Zimm plots. In the following, the values of  $R_g$ ,  $R_H$ , and  $M_w$  determined for the two populations of molecules present in the renatured scleroglucan solutions are compared with values obtained for circular and linear structures of scleroglucan determined using other techniques. The correspondence between the values obtained and those expected for circular and linear structures is found to be within a

physically reasonable range in view of the heterogeneity of the samples. The two populations of molecules present in the renatured scleroglucan sample detected using the combined dynamic and static light scattering approach are thus identified as the circular and linear morphologies of scleroglucan.

Aggregates sometimes form during the scleroglucan renaturation process. Such aggregates would show a slow diffusion and would thus offer an alternative interpretation of the bimodal DLS spectrum. Aggregate formation would lead to an increase in the  $M_w$  values of the samples. The SEC-MALLS studies performed on the same sample revealed that the denaturation–renaturation treatment of this sample led only to a small increase (4.5%) in  $M_w$ , which indicates that the number of aggregates present in this solution is low. This number is expected to be even lower in the solution studied by light scattering owing to the different filtering procedure employed. Prior to the DLS measurements, filters with a pore size of 0.2  $\mu\text{m}$  were used, whereas prior to injection into the SEC-MALLS column, filters with a pore size of 0.8  $\mu\text{m}$  were used. This interpretation is consistent with the information extracted from AFM topographs (Figure 2B), in which only a small fraction of overlapping linear chains can be seen in the images, and the DLS spectra, in which no separate high  $M_w$  population is observed.

The SEC-MALLS chromatograms show overlap in the elution volume of the two classes of species, that is, circular and linear structures.<sup>16</sup> The overlap makes it difficult to directly determine the molecular weight of the circular and linear structures separately using SEC-MALLS. For the linear structures, this can be overcome by measuring a sample containing only linear structures, that is, one not exposed to a denaturation–renaturation cycle. In such a sample studied by SEC-MALLS, the value found for  $M_w$  was  $4.2 \times 10^5$ , which, within experimental error, is identical to that determined by SLS, that is,  $3.9 \times 10^5$  g/mol. The determination of  $M_w$  for the circular fraction of molecules is more difficult owing to the lack of a sample containing only circular molecules. In a previous work, the elution profiles of samples with different relative contents of circular structures were compared (Figure 4).<sup>16</sup> The circular structures eluted mainly between 20 and 28 mL. In this work,  $M_w$  for the circular molecules eluting in the intervals 21–22, 22–23, and 23–24 mL was also determined. Its value decreased from  $5.8 \times 10^5$  to  $4.4 \times 10^5$  to  $3.5 \times 10^5$  g/mol. Since these three intervals were in the high  $M_w$  part of the elution interval for the circular structures,  $3.2 \times 10^5$  g/mol seems to be a reasonable estimate for  $M_w$  for the total population of circular molecules. An increase of 5% in the number fraction of circular structures, estimated to be 50%, incurs a change of  $-8$  and  $+12\%$  in the  $M_w$  values of the circular and linear species, respectively. This example illustrates how inaccuracies of a few percent in the relative concentration of circular structures influence the  $M_w$  value determined by light scattering.

An important characteristic of this sample for the analysis of the light scattering data is its polydispersity. After renaturation, the polydispersity index of the sample increased from  $1.4 \pm 0.1$  to  $1.6 \pm 0.05$ . For the scleroglucan samples, a spread in molecular weight of the populations of both the circular and linear fractions is expected. Polydispersity does influence  $R_H$ , since, when evaluating  $D_T$  on the basis of the initial portion of the autocorrelation function, the value obtained will be the  $z$ -average. Since  $R_H$  is inversely proportional to  $D_T$ , the fast diffusing structures will within each of the two populations of particles have more impact on the values obtained for  $R_H$  than the more slowly diffusing structures. The situation is further complicated by the fact that  $R_{H,\text{app}}$  is not an approximation of

$\langle R_H \rangle_z$  because  $1/\langle D \rangle_z \neq \langle 1/D \rangle_z$ . This influence on  $R_H$  can be corrected for,<sup>33</sup> but the influence of polydispersity on the radius of gyration is expected to be much more severe.<sup>34</sup> In the following, we have therefore chosen to correct for the influence of polydispersity on  $R_g$ , but not on  $R_H$ . Polydispersity may explain the relatively high values found for  $R_g$ , since this parameter, determined from a Zimm plot, is a  $z$ -average. It has previously been noted that discrepancies between the experimental results from different groups on the  $z$ -average radius of gyration and weight-average molecular weights are associated with differences in the molecular weight heterogeneity.<sup>32</sup> The polydispersity should therefore be taken into account before comparing our results to those from studies of solutions with a polydispersity index close to 1. The influence of polydispersity on  $R_g$  can be evaluated from the relations  $M_{z+1}/M_z = M_z/M_w = M_w/M_n$ , where  $M_z$  and  $M_{z+1}$  are the  $z$  and  $z + 1$  average of the molecular weight and  $M_w/M_n$  is determined experimentally. On the basis of this approach and the polydispersity of the mixture determined by SEC-MALLS, a radius of gyration of approximately 90 nm is expected for this mixture. This value is lower than the value determined by light scattering (Table 2). This difference can be explained by an underestimation of the polydispersity of the linear fraction of the renatured scleroglucan solution.

Turning to the circular fraction,  $R_g$  was found to be 41 nm. Previously,  $M_w$  and  $R_g$  for circular structures as they eluted from a gel filtration column were determined.<sup>16</sup>  $M_w$  and  $R_g$  were determined for three selected fractions in the center of the broad peak where the circular structures eluted. The three fractions showed an increase in  $M_w$  from  $3.5 \times 10^5$  to  $5.8 \times 10^5$  g/mol and a corresponding increase in  $R_g$  from 26 to 42 nm. The value of  $R_g = 41$  nm determined here is therefore in accordance with the value previously determined for the circular structures. On the basis of the AFM image (Figure 2B), it can be concluded that the population of circular structures is also polydisperse, giving rise to circular structures of differing radii. The polydispersity for this population is however limited by the chain length dependence of the ring forming capacity.<sup>15</sup> The overestimate of  $R_g$  due to polydispersity is therefore, for the circular fraction, limited by chain length requirements inherent to the ring formation process. In a mixture of particles having different diffusion times, there is however a possibility that the fast component includes some contribution of the slow component, which also will tend to increase the apparent value of  $R_g$  (small);  $R_H$ , however, is less affected.

Depolarized light scattering was performed in an attempt to obtain information concerning the rotational diffusion coefficient of the molecules. This parameter is sensitive to the effective length and geometry of the polymer. The signal was, however, too weak to give meaningful results.

Additional structural information about the linear and circular fractions is obtained by calculating the ratio of the two radii,  $\rho = R_g/R_H$ . The calculation gives  $\rho = 2.7 \pm 0.5$  for the circular structures and  $\rho = 1.50 \pm 0.25$  for the linear structures.  $\rho$  is a structure-sensitive dimensionless parameter that can be used as a qualitative measure of the main macromolecular architecture in the solution. Values of  $\rho$  expected for different structures have been reported.<sup>35</sup> For rigid structures, a logarithmic growth with the contour length is predicted. For the rod and the rigid ring, behavior described by the following two equations is predicted:<sup>36</sup>

$$\rho_{\text{rod}} = (\ln N - 1)/3^{1/2} \quad (3)$$

$$\rho_{\text{ring}} = (\ln N - 0.45)/\pi \quad (4)$$



In these equations,  $N$  denotes the number of bonds per chain.  $N$  is used here in order to reflect the contour length of the chains. For a triple helical polymer having side chains attached to every third unit, as is the case for scleroglucan, the number of bonds does not directly reflect the contour length. After correction for the effect of the side chains and the helical structure,  $N = 184$  is obtained, which yields  $\rho$  equal to 1.51 and 2.42 for the circular and linear fractions, respectively. The  $\rho$  value obtained clearly indicates that the linear molecules do not exhibit the behavior expected for stiff rodlike structures. For stiff rodlike polymers, values of  $\rho$  that are smaller than predicted by eq 3 have previously been observed.<sup>37</sup> A possible explanation for the observed deviation is that stiff polymers behave as perfect linear arrays; that is, they obey eq 3, only when the chain length is equal to or smaller than one Kuhn segment. To illustrate this point, we adopt the model of Perrin<sup>38</sup> in which the linear segment is approximated by a prolate ellipsoid of revolution with aspect ratio  $a/b = 100$ , corresponding to the ratio of the persistence length to the diameter of the scleroglucan triple helix. From Perrin's expression for  $R_H$  and the standard formula for the radius of gyration of an ellipsoid of revolution,  $\rho = 2.36$ . To attain  $\rho = 1.50 \pm 0.25$ , the aspect ratio must be in the interval 8–25, with a value equal to 14 at  $\rho = 1.50$ . A similar conclusion is obtained from the calculation of Tirado for a cylinder of length  $L$  and radius  $R$ .<sup>39</sup> The effective aspect ratio is reduced, however, if the rods can bend. Inspection of the AFM image presented in Figure 2B indeed reveals that a significant fraction of the linear chains have defects in the form of loops or side chains larger than single glucose residues. Such deviations from linearity of the chains could explain the results in this particular case of renatured scleroglucan. These deviations arise as a result of the renaturation process, where a fraction of the single chains come together upon renaturation to form structures that are not perfect triple helical linear structures. This has previously been observed in mixtures of renatured triple helical (1 $\rightarrow$ 3)- $\beta$ -D-glucans where the structures were fractionated on the basis of their hydrodynamic properties. In the fractions containing the largest structures, star-shaped and irregularly branched structures were observed.<sup>40</sup> For such irregular structures, a value of  $\rho$  close to unity is expected.<sup>35</sup> This conclusion was strengthened by measurements performed on linear scleroglucan that had not been exposed to a denaturation–renaturation cycle and which yielded  $\rho = 1.9$  (data not shown).

## Conclusions

Light scattering observations performed on a sample of scleroglucan exposed to denaturing conditions, then renatured, revealed that the sample is a mixture of two populations of molecules with different hydrodynamic radii. Zimm plots prepared for each of the fractions making up the mixture allowed the determination of  $M_w$  and  $R_g$  for each separate population. The values obtained are in good agreement with those previously determined for linear and circular morphologies of (1 $\rightarrow$ 3)- $\beta$ -D-glucan present in this or similar samples, despite the complications due to a spread of geometries and molar masses of the molecules present in this sample. Apparent discrepancies between the values obtained using light scattering and those obtained using other techniques can be explained by the properties of the sample as measured by the DLS and SLS techniques. The results show that DLS or a combination of DLS and SLS can afford fast and reliable structural information concerning individual subpopulations present in these mixtures.

SEC has previously been used to investigate the structural changes in scleroglucan samples exposed to a denaturation–renaturation treatment.<sup>15,16</sup> In those studies, the partial overlap in the elution profile of circular and linear structures prevented a precise direct determination of the fraction of circular structures at each elution volume. Innovations in high speed electronic components such as high performance diode lasers, high speed digital signal processors, and photodiode detectors have led to the evolution of a flow-mode DLS detector, which has been used for “on-the-fly” determination of the  $R_H$  values of biomolecules eluting from SEC columns.<sup>41</sup> The results presented in this paper show that addition of such a DLS detector to the outlet of a SEC column would provide additional information regarding the morphology of the structures and can therefore yield a precise determination of the fraction of circular structures using SEC-MALLS.

**Acknowledgment.** The authors thank Cyrille Rochas of the Laboratoire de Spectrométrie Physique, Université Joseph Fourier de Grenoble, France, for helpful discussions and engineer Ann-Sissel Ulset, Department of Biotechnology, NTNU, Norway, for carrying out the phenol–sulfuric acid reaction. M.S. is grateful for the hospitality shown by the members of “Spectro” in Grenoble during the spring semester 2004. This work was supported by the Norwegian Research Council Grant No. 145523/432.

## References and Notes

- (1) Johnson, J.; Kirkwood, S.; Misaki, A.; Nelson, T. E.; Scaletti, J. V.; Smith, F. *Chem. Ind.* **1963**, 820–822.
- (2) Norisuye, T.; Yanaki, T.; Fujita, H. *J. Polym. Sci., Polym. Phys. Ed.* **1980**, *18*, 547–558.
- (3) Yanaki, T.; Kojima, T.; Norisuye, T. *Polym. J.* **1981**, *13*, 1135–1143.
- (4) Gawronski, M.; Aguirre, G.; Conrad, H.; Springer, T.; Stahmann, K.-P. *Macromolecules* **1996**, *29*, 1516–1520.
- (5) Yanaki, T.; Norisuye, T.; Fujita, H. *Macromolecules* **1980**, *13*, 1462–1466.
- (6) Sato, T.; Teramoto, A. *Macromolecules* **1991**, *24*, 193–196.
- (7) Bluhm, T. L.; Deslandes, Y.; Marchessault, R. M.; Perez, S.; Rinaudo, M. *Carbohydr. Res.* **1982**, *100*, 117–130.
- (8) Tabata, K.; Ito, W.; Kojima, T.; Kawabata, T.; Misaki, A. *Carbohydr. Res.* **1981**, *89*, 121–135.
- (9) Kitamura, S.; Kuge, T. *Biopolymers* **1989**, *28*, 639–654.
- (10) Yanaki, T.; Tabata, K.; Kojima, T. *Carbohydr. Polym.* **1985**, *5*, 275–283.
- (11) Aasprong, E.; Smidsrød, O.; Stokke, B. T. *Biomacromolecules* **2003**, *4*, 914–921.
- (12) Stokke, B. T.; Elgsaeter, A.; Brant, D. A.; Kuge, T.; Kitamura, S. *Biopolymers* **1993**, *33*, 193–198.
- (13) Stokke, B. T.; Elgsaeter, A.; Brant, D. A.; Kitamura, S. *Macromolecules* **1991**, *24*, 6349–6351.
- (14) McIntire, T. M.; Brant, D. A. *J. Am. Chem. Soc.* **1998**, *120*, 6909–6919.
- (15) Falch, B.; Elgsaeter, A.; Stokke, B. T. *Biopolymers* **1999**, *50*, 496–512.
- (16) Sletmoen, M.; Christensen, B. E.; Stokke, B. T. *Carbohydr. Res.* **2005**, *340*, 971–979.
- (17) Falch, B. H.; Stokke, B. T. *Carbohydr. Polym.* **2001**, *44*, 113–121.
- (18) Stokke, B. T.; Elgsaeter, A.; Kitamura, S. *Int. J. Biol. Macromol.* **1993**, *15*, 63–68.
- (19) Stacey, K. A. *Light Scattering in Physical Chemistry*; Butterworth Scientific Publications: London, 1956.
- (20) Huglin, M. B. Specific refractive index increments. In *Light scattering from polymer solutions*; Huglin, M. B., Ed.; Academic Press: London and New York, 1972; pp 163–331.
- (21) Hiemenz, P. C.; Rajagopalan, R. In *Principles of Colloid and Surface Chemistry, Revised and Expanded*, 3rd ed.; Marcel Dekker Inc.: New York, 1997; 193–247.
- (22) Berne, B. J.; Pecora, R. *Dynamic light scattering*, John Wiley & Sons: New York, 1975.
- (23) Benmouna, M.; Benoit, H.; Duval, M.; Akcasut, Z. *Macromolecules* **1987**, *20*, 1107–1112.

- (24) Akcasu, A. Z.; Hammouda, B.; Lodge, T. P.; Han, C. *Macromolecules* **1984**, *17*, 759–766.
- (25) Corrotto, J.; Ortega, F.; Vazquez, M.; Freire, J. J. *Macromolecules* **1996**, *29*, 5948.
- (26) Provencher, S. W. *Comput. Phys. Commun.* **1982**, *27*, 213–227.
- (27) Provencher, S. W. *Comput. Phys. Commun.* **1982**, *27*, 229–242.
- (28) Liu, T.; Rulkens, R.; Wegner, G.; Chu, B. *Macromolecules* **1998**, *31*, 6119–6128.
- (29) Dubois, M.; Gilles, K. A.; Hamilton, J. K.; Rebers, P. A.; Smith, F. *Anal. Chem.* **1956**, *28*, 350–356.
- (30) Stokke, B. T.; Falch, B. H.; Dentini, M. *Biopolymers* **2001**, *58*, 535–547.
- (31) Sun, C. D.; Wang, Z.; Wu, G.; Chu, B. *Macromolecules* **1992**, *25*, 1114.
- (32) Kashiwagi, Y.; Norisuye, T.; Fujita, H. *Macromolecules* **1981**, *14*, 1220–1225.
- (33) Wu, C. *Colloid Polym. Sci.* **1993**, *271*, 947–951.
- (34) Harnau, L.; Winkler, R. G.; Reineker, P. *Macromolecules* **1999**, *32*, 5956–5960.
- (35) Burchard, W. *Adv. Polym. Sci.* **1999**, *143*, 113–194.
- (36) Burchard, W. Theory of cyclic macromolecules. In *Cyclic polymers*; Semlyen, J. A., Ed.; Elsevier Applied Science Publishers: London and New York, 1986; pp 43–84.
- (37) Coviello, T.; Kajiwar, K.; Burchard, W.; Dentini, M.; Crescenzi, V. *Macromolecules* **1986**, *19*, 2826–2831.
- (38) Perrin, F. *J. Phys. Radium* **1936**, *7*, 1936.
- (39) Tirado, M. M.; Garcia de la Torre, J. *J. Chem. Phys.* **1979**, *71*, 2581–2587.
- (40) Stokke, B. T.; Elgsaeter, A.; Kitamura, S. *Polym. Gels Networks* **1994**, *2*, 173–190.
- (41) Liu, Y.; Bo, S.; Zhu, Y.; Zhang, W. *Polymer* **2003**, *44*, 7209–7220.

BM050990M